Feasibility Study of Inductor Coupling in Three-Level Neutral-Point-Clamped Quasi-Z-Source DC/AC Converter

Janis Zakis, *Member*, *IEEE*, Oleksandr Husev, *Member*, *IEEE*, and
Ryszard Strzelecki, *Senior Member*, *IEEE*

***Abstract*—This paper presents a comparative feasibility study of coupled inductor implementation in a three-level neutral-point-clamped quasi-Z-source (3L-NPC qZS) DC/AC converter. Our theoretical verification shows that coupling of the qZS inductors enables reductions in the size and weight of the magnetic components or in the input current ripple. Our mathematical analysis shows the difference of inductor currents at variable circuit parameters. Simulations results are provided to verify our theoretical assumptions.**

***Index Terms*—DC/AC converter, three-level inverter, coupled inductors, quasi-Z-Source.**

I. Introduction

Recent studies have shown that three-level neutral point clamped quasi-Z-source inverter (3L NPC qZSI) based DC/AC converter performance is effective and reliable [1]–[4]. Fig. 1 illustrates a general circuit diagram of the 3L NPC qZSI based single-phase DC/AC converter. The main advantages of the converter are continuous input current, input voltage preregulation in the single stage and shoot-through immunity as compared to similar topologies. Unfortunately due to the large number of passive components of both qZS-networks (L_1, L_2, C_1, C_2, D_1 and L_3, L_4, C_3, C_4, D_2), the size and weight of the overall 3L NPC qZSI are relatively large. This leads to a need for optimization or reduction of passive components.

In some cases, implementation of coupled inductors (two inductors on one magnetic core) is an effective solution to reduce the number of turns in the windings due to the flux doubling effect. Also, if the numbers of turns remains the same, then the inductor current ripple as well as the input current ripple can be reduced [5]–[9].

This paper presents an analytical and simulation study of integration possibilities of the qZS-network magnetic elements in order to reduce the dimensions of the overall converter. At the same time, the main electric parameters of the converter should remain the same as those with single magnetic components.

This research work has been supported by Latvian Council of Science (Grant 673/2014) and Postdoctoral Research Grant (MJD391).

J. Zakis is with the Institute of Industrial Electronics and Electrical Engineering, Riga Technical University, Kronvalda 1, LV1010, Riga, (e-mail: janis.zakis@ieee.org).

O. Husev is with the Department of Electrical Engineering, Tallinn University of Technology, Ehitajate tee 5, 19086 Tallinn, Estonia (e-mail: oleksandr.husev@ieee.org).

R. Strzelecki is with the Department of Electrotechnics and Precision Electromechanical Systems, ITMO University 197101, St.Petersburg, Kronverkskiy pr, 49 (e-mail: rstrzele@am.gdynia.pl) and Electrotechnical Institute, 04-703 Warsaw, ul. Pożaryskiego 28
(email: r.strzelecki@iel.waw.pl).

©2014 IEEE

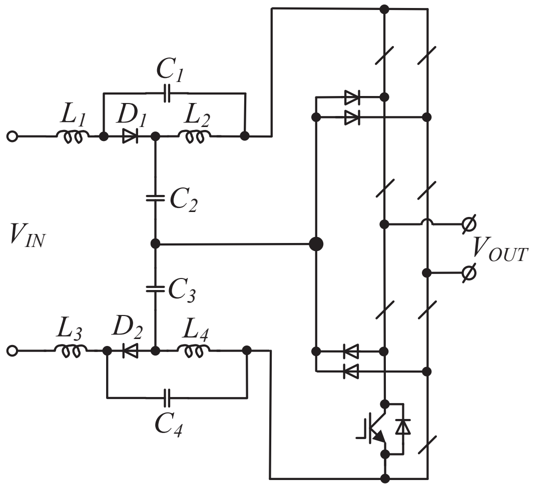

Fig. 1. General circuit diagram of the single phase three-level neutral-point-clamped quasi-Z-source inverter (3L-NPC qZSI).

II. Mathematical Analysis of Inductor Coupling

To reduce the physical parameters of the proposed 3L NPC qZSI (Fig. 1), several combinations of inductor coupling can be considered.

Fig. 2 demonstrates a typical waveform of the DC-link current. It is evident that it contains direct and alternative components. The fundamental harmonic of the alternative component can be easily estimated by help of the Fourier analysis:

$$\dot{I}_{dc} = \frac{\sqrt{2}\cdot 4}{3\pi}\frac{P_{out}}{V_{out}}\sin(2\omega t)\,. \quad (1)$$

At the same time, this current flows through the qZS-network and evokes low frequency oscillation in the inductors. This current ripple strictly depends on the passive components and on inductor coupling in particular.

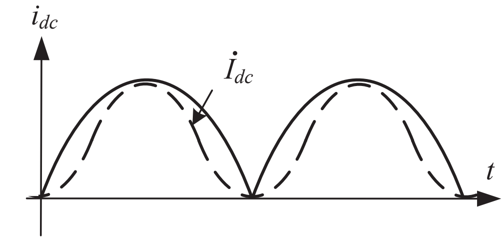

Fig. 2. DC-link current waveform.

Figs. 3 and 5 present equivalent circuits of a general circuit diagram with different inductor coupling possibilities. In both diagrams (Figs. 3 and 5) the inverter is substituted with a sinusoidal current source that corresponds to the first harmonic component of the current consumed by the inverter. The inverter is the only source of low frequency current ripple in the system. For the circuit analysis, the linearized model of a symmetric qZS network is used. Since the inverter is the only source of low frequency current ripple, we can apply the reduced superposition theorem and complex impedance to analyze the AC behavior of the circuit.

The main parameters under investigation in both coupling cases are the fundamental components of the alternative currents (current ripple) $\dot{I}_{L1}$ and $\dot{I}_{L2}$ of inductors L_1 and L_2, respectively.

A. Coupling of Inductors L_1 With L_3 and L_2 With L_4

Fig. 3 presents a simplified equivalent circuit of the proposed converter where inductors L_1 with L_3 and L_2 with L_4 are coupled. The inverter is substituted with the current source $\dot{I}_{dc}$ and the active resistance of the contour is R that also includes the active resistance of the inductor winding.

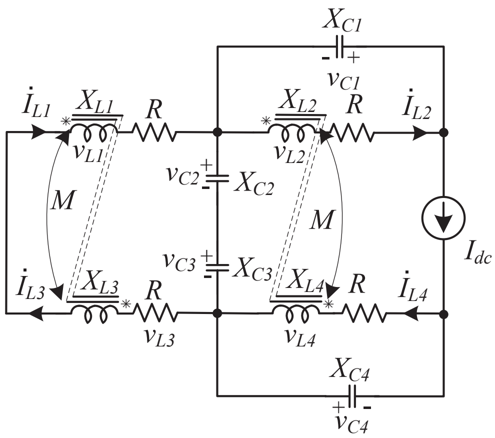

Fig. 3. Equivalent circuit of the 3L NPC qZSI when L_1 is coupled with L_3 and L_2 is coupled with L_4.

Such coupling does not have any effect on the current, therefore the currents in the coupled inductors are equal. In this case basic equations can be expressed as

$$\begin{cases} \dot{I}_{dc} = \dot{I}_{L2} + \dot{I}_{C1} \\ \dot{I}_{dc} = \dot{I}_{L1} + \dot{I}_{C2} \\ \dot{I}_{L2} \cdot x_{L2} + \dot{I}_{L2} \cdot R = \dot{I}_{C1} \cdot x_{C1} \\ \dot{I}_{L1} \cdot x_{L1} + \dot{I}_{L1} \cdot R = \dot{I}_{C2} x_{C2} \end{cases}, \quad (2)$$

Fig. 4 shows the fundamental harmonic AC current peak values of both inductors (L_1 and L_2) $\dot{I}_{L1}$ and $\dot{I}_{L2}$. Curves were obtained at the following circuit parameters ($P = 1$ kW, $V_{OUT} = 230$ V, $C_1 = 200$ µF, $C_2 = 600$ µF, $R = 0.1$ Ω, and $L_1 = L_2 = L_3 = L_4 = 20 \ldots 2000$ µH).

The figure shows that in the selected range of inductances of the qZS network, inductors are possible resonant cases (at 200 µH and 600 µH) that should be taken into account. Further increasing of the inductance leads to a decrease in the current ripples.

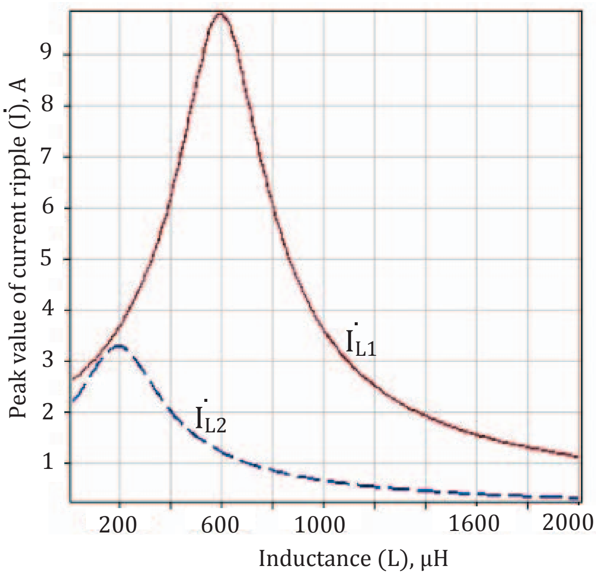

Fig. 4. Peak current $\dot{I}_{L1}$ and $\dot{I}_{L2}$ values of fundamental harmonics ripple depending on the inductor inductances ($L_1 = L_2 = 20 \ldots 2000$ µH) without coupling.

Current ripple in the first inductor is greater than in the second one. It is explained by different values of the capacitance of capacitors C_1 and C_2.

B. Coupling of Inductors L_1 With L_2 and L_3 With L_4

Fig. 5 presents a simplified equivalent circuit of the proposed converter if inductors L_1 with L_2 and L_3 with L_4 are coupled. Similarly to Fig. 3, the inverter is substituted with the current source I_{dc}.

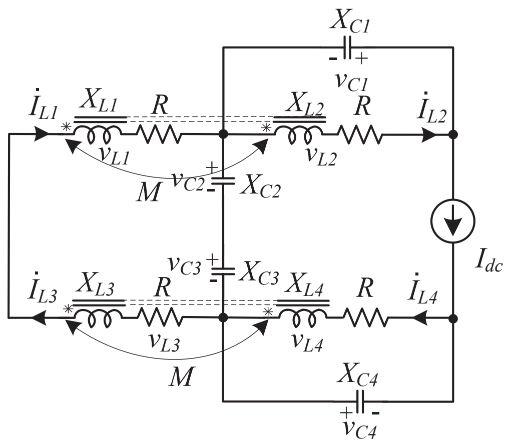

Fig. 5. Equivalent circuit of the 3L NPC qZSI when L_1 is coupled with L_2 and L_3 is coupled with L_4.

General equations that characterize the circuit diagram in Fig. 5 can be expressed as follows:

$$\begin{cases} \dot{I}_{dc} = \dot{I}_{L2} + \dot{I}_{C1} \\ \dot{I}_{dc} = \dot{I}_{L1} + \dot{I}_{C2} \\ R\dot{I}_{L2} + \dot{I}_{L2} \cdot x_{L2} + \dot{I}_{L1} \cdot x_M = \dot{I}_{C1} \cdot x_{C1} \\ R \cdot \dot{I}_{L1} + \dot{I}_{L1} x_{L1} + \dot{I}_{L2} \cdot x_M = \dot{I}_{C2} x_{C2} \end{cases} \quad (3)$$

Fig. 6 presents the peak current $\dot{I}_{L1}$ and $\dot{I}_{L2}$ ripples of the fundamental harmonic obtained from the equation system (3) that depend on the inductance of both inductors (L_1 and L_2). The circuit parameters are the same as previously ($P = 1$ kW, $V_{OUT} = 230$ V, $C_1 = 200$ µF, $C_2 = 600$ µF, $R = 0.1$ Ω, and $L_1 = L_2 = 20\ldots1000\ \mu$H), with the exception that in this case also mutual inductance M is playing a role and is accepted similarly to the inductance of inductors ($L_1 = L_2 = L_3 = L_4 = M$). It corresponds to the full coupling between the inductors. Total magnetic resistance is equivalent to the previous case.

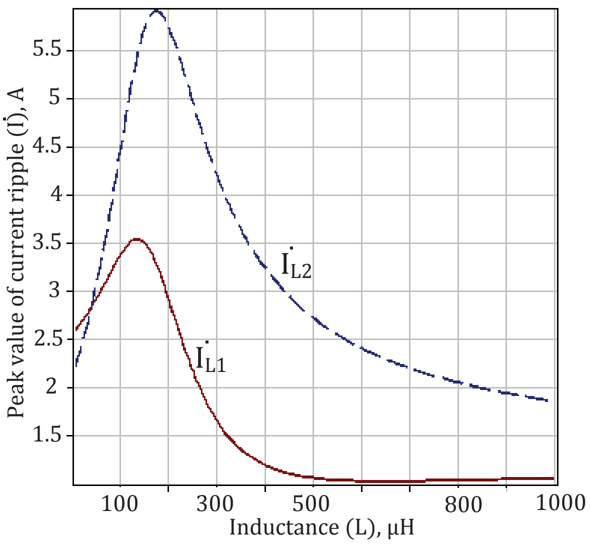

Fig. 6. Peak current $\dot{i}_{L1}$ and $\dot{i}_{L2}$ values of fundamental harmonics ripple depending on the inductor and the mutual inductances ($L_1 = L_2 = M =$ 20..1000 µH).

It can be seen that the resonance phenomenon is slightly mitigated as compared to a non-coupling design. At the same time, current ripple in the second inductor is greater than in the first one. But the overall current ripple in both inductors is significantly decreased.

Fig. 7 shows the peak current $\dot{i}_{L1}$ and $\dot{i}_{L2}$ ripples of the fundamental harmonic at the constant circuit parameters ($P = 1$ kW, $V_{OUT} = 230$ V, $C_1 = 200\ \mu$F, $C_2 = 600\ \mu$F, $R = 0.1\ \Omega$ and $L_1 = L_2 = 400\ \mu$H) and variable mutual inductance ($M = 0\ldots400\ \mu$H).

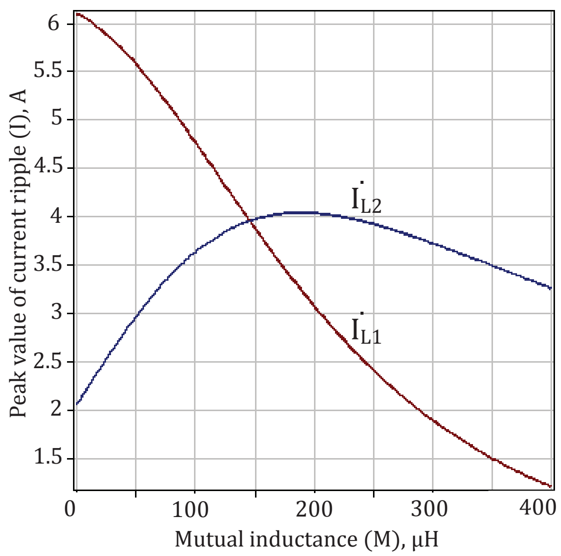

Fig. 7. Peak current $\dot{i}_{L1}$ and $\dot{i}_{L2}$ values of fundamental harmonics ripple depending on the constant inductance of inductors ($L_1 = L_2 = 400$ µH) and variable mutual inductance ($M = 0\ldots400$ µH).

This picture shows how mutual inductance influences the current ripple in the inductors.

III. Simulation Results

To verify our mathematical analysis, the 3L NPC qZSI model in PSIM simulation software was developed and the discussed different combinations of the coupled inductors were verified. The converter operation in both discussed cases was accepted in the continuous conduction mode (CCM).

A. Coupling of Inductors L_1 With L_3 and L_2 With L_4

Fig. 8 presents the currents of inductors L_1 and L_2. As it was expected, the input current fluctuates at the two fold grid frequency (100 Hz).

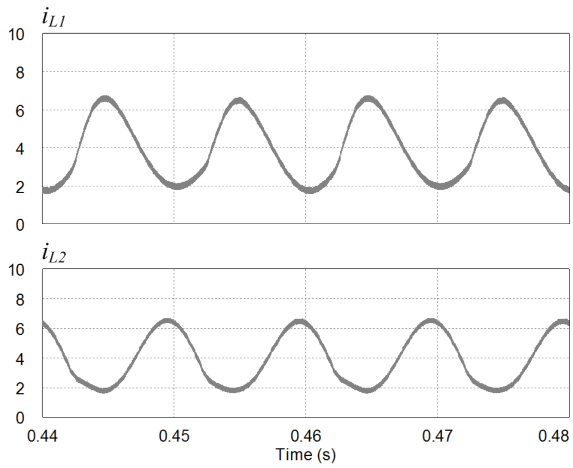

Fig. 8. Current i_{L1} and i_{L2} of inductors L_1 and L_2, respectively.

The circuit parameters of the simulation model are as follows: inductance of inductors (L_1, L_2, L_3, L_4) was taken 5 mH, mutual inductance 0 H, capacitance of capacitors $C_1 = C_3 = 600\ \mu$F, $C_2 = C_4 = 200\ \mu$F, input voltage 200 V, and the *rms* value of the output voltage 230 V. The discussed converter works in the voltage boost mode with a shoot-through duty cycle $D_S = 0.13$.

B. Coupling of Inductors L_1 With L_2 and L_3 With L_4

Fig. 9 presents the currents of inductors L_1 and L_2. The circuit parameters of the simulation model are as follows: inductance of inductors (L_1, L_2, L_3, L_4) was taken 2.5 mH mutual inductance 2.499 mH (99% coupling), capacitance of capacitors $C_1 = C_3 = 600\ \mu$F, $C_2 = C_4 = 200\ \mu$F, input voltage 200 V and the *rms* value of the output voltage 230 V. Similarly to the previous case, the discussed converter works in the voltage boost mode with a shoot-through duty cycle $D_S = 0.13$.

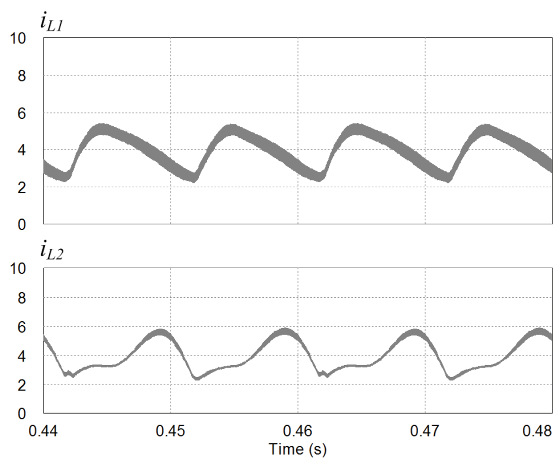

Fig. 9. Current i_{L1} and i_{L2} of inductors L_1 and L_2, respectively.

Table I presents high and low frequency harmonics of the inductor currents (i_{L1} and i_{L2}) in both coupling cases. It can be seen that in the case of coupling of inductors L_1 with L_2 and L_3 with L_4, the difference in the current ripple of i_{L1} and i_{L2} low frequency harmonics is larger.

TABLE I. FAST FOURIER TRANSFORM

Current	Frequency				
	100 Hz	**25 kHz**	**50 kHz**	**75 kHz**	**100 kHz**
	Coupling of Inductors L1 with L3 and L2 with L4				
i_{L1}, (A)	2.33	0.125	0.041	0.011	0.002
i_{L2}, (A)	2.4	0.129	0.043	0.012	0.002
	Coupling of Inductors L1 with L2 and L3 with L4				
i_{L1}, (A)	1.1	0.285	0.057	0.012	0.003
i_{L2}, (A)	1.33	0.091	0.045	0.014	0.001

IV. CONCLUSION

This paper presents theoretical analysis of the inductor coupling of the 3L-NPC qZS converter.

Mathematical results show that coupling combinations influence the low frequency current ripple significantly. Also, resonant conditions are different in both coupling combinations.

Simulation results proved our mathematical assumptions. In the second variant of coupling, the current ripple decreased substantially and therefore it is preferable for use since the total inductance is the same.

At the same time, some differences between the analytical and simulation results can be explained by the nonlinear behavior of the converter and our simplified analytical model.

Focus in our future work will be on the development of an experimental setup and experimental verification of theoretical results.

REFERENCES

[1] O. Husev, S. Stepenko, C.Roncero-Clemente, E. Romero-Cadaval, and D. Vinnikov, “Single-phase three-level quasi-Z-source inverter with a new boost modulation technique,” *Proceedings of IECON 2012 – 38th Annual Conference on IEEE Industrial Electronics Society*, pp. 5856-5861, Montreal, Canada, October 25-28, 2012.

[2] O. Husev, C. Roncero-Clemente, S. Stepenko, D. Vinnikov, and E. Romero-Cadaval, “CCM operation analysis of the single-phase three-level quasi-Z-source inverter,” *In: Proceedings of 15th International Power Electronics and Motion Control Conference and Exposition, EPE-PEMC 2012*, September 4-6, 2012.

[3] S. Stepenko, O. Husev, D. Vinnikov, and S. Ivanets, “FPGA control of the neutral point clamped quasi-Z-source inverter,” *Proceedings of the 13th Biennial Baltic Electronics Conference (Tallinn, Estonia, 3–5 October 2012). – Tallinn: TUT,* 2012. – pp. 263-266.

[4] C. Roncero-Clemente, O. Husev, V. Minambres-Marcos, E. Romero-Cadaval, S. Stepenko, and D. Vinnikov, “Tracking of MPP for three-level neutral-point-clamped qZ-source off-grid inverter in solar applications,” *Journal of Microelectronics, Electronic Components and Materials Vol. 43, No. 4 (2013)*, pp. 212–221.

[5] Y. Li, J. Anderson, F. Z. Peng, and D. Liu, "Quasi-Z-source inverter for photovoltaic power generation systems," *Twenty-Fourth Annual IEEE Applied Power Electronics Conference and Exposition APEC 2009*, pp. 918–924, 15–19 Feb. 2009.

[6] G. Zhu, B. A. McDonald, and K. Wang, "Modeling and analysis of coupled inductors in power converters," *Twenty-Fourth Annual IEEE Applied Power Electronics Conference and Exposition, APEC 2009*, pp. 83–89, 15–19 Feb. 2009.

[7] J. Zakis, D. Vinnikov, and L. Bisenieks, “Some design considerations for coupled inductors for integrated buck-boost converters,” *III International Conference on Power Engineering, Energy and Electrical Drives POWERENG 2011*, pp. 1–6, 2011.

[8] G. Zhu, B. A. McDonald, and K. Wang, "Modeling and analysis of coupled inductors in power converters," *IEEE Transactions on Power Electronics*, vol.26, no.5, pp.1355–1363, May 2011.

[9] H.-B Shin, J.-G Park, S-K. Chung, H.-W Lee, and T. A. Lipo, "Generalised steady-state analysis of multiphase interleaved boost converter with coupled inductors," *Electric Power Applications, IEE Proceedings*, vol. 152, no. 3, pp. 584–594, 6 May 2005.

BIOGRAPHIES

Janis Zakis (M’10) received B.Sc., M.Sc. and Dr.Sc.ing. degrees in electrical engineering from Riga Technical University, Riga, Latvia, in 2002, 2004 and 2008, respectively.

He is presently a Senior Researcher in the Institute of Industrial Electronics and Electrical Engineering, Riga Technical University.

He has over 30 publications and is the holder of one Utility Model in power converter design. His research interests include flexible ac transmission systems (FACTS), simulation of power systems, switching mode power converters, applied design of power converters and energy storage systems.

Oleksandr Husev received the B.Sc. and M.Sc. degrees in industrial electronics from Chernihiv State Technological University, Chernihiv, Ukraine, in 2007 and 2008, respectively. He defended his Ph.D. thesis in the Institute of Electrodynamics of the National Academy of Science of Ukraine in 2012.

He is Senior Researcher of the Department of Electrical Engineering, Tallinn University of Technology and Assistant of the Department of Biomedical Radioelectronics Apparatus and Systems, Chernihiv State Technological University. He has over 40 publications and is the holder of several patents.

His research interests are in control systems for power electronic converters based on a wide range of algorithms, including modeling, design, and simulation, applied design of power converters and control systems and application.

Ryszard Strzelecki (M’97–SM’07) was born in Bydgoszcz, Poland. He received the M.Sc. (with honors) and Ph.D. degrees in electronic engineering from the Department of Industrial Electronics, National Technical University of Ukraine “Kyiv Polytechnic Institute,” Kyiv, Ukraine, in 1981 and 1984, respectively, and the Dr.Sc. degree in electrical engineering from the Institute of Electrodynamics, The National Academy of Sciences of Ukraine, Kyiv, in 1991. From 1996 to 2003, he was the Director of the Institute of Electrical Engineering, University of Zielona Góra, Zielona Góra, Poland. He is currently a Contractes Profesor with the Department of Electrotechnics and Precision Electromechanical Systems, ITMO University (St. Petersburg, Russia) and Full Professor with the Power Electronics Laboratories of Electrotechnical Institute (Warsaw, Poland) and Gdynia Maritime University (Gdynia, Poland).

His research activity is centered on the topology, control, and industry application of power electronic conditioners, particularly for power quality enhancement and power flow control on distributed electrical networks. He is the author of numerous technical papers and six books and monographs and the holder of six patents. He is a Member of the Editorial Boards of the journals *Electrical Power Quality and Utilization* and *Przegląd Elektrotechniczny (Electrical Review)*. Dr. Strzelecki is the Chair of the Power Electronics Committee of the Association of Polish Electrical Engineers. He is the Founder and currently a Cochairman of the IEEE Conference-Workshop Compatibility and Power Electronics.

This is a post-print of a paper published in 2014 Electric Power Quality and Supply Reliability Conference (PQ) Proceedings [http://dx.doi.org/PQ.2014.6866826] and is subject to IEEE copyright.